

# Modeling atmospheric effects of the September 1859 Solar Flare

B . C . Thom as

Department of Physics and Astronomy, Washburn University, Topeka, Kansas, USA

C . H . Jackm an

Laboratory for Atmospheres, NASA Goddard Space Flight Center, Greenbelt, Maryland, USA

A . L . M elott

University of Kansas, Department of Physics and Astronomy, Lawrence, Kansas, USA

We have modeled atmospheric effects, especially ozone depletion, due to a solar proton event which probably accompanied the extreme magnetic storm of 1–2 September 1859. We use an inferred proton fluence for this event as estimated from nitrate levels in Greenland ice cores. We present results showing production of odd nitrogen compounds and their impact on ozone. We also compute rainout of nitrate in our model and compare to values from ice core data.

## 1. Introduction

Atmospheric ozone effects by solar proton events (SPEs) associated with solar eruptive events have been studied since the 1970's. Ozone depletion occurs following the production of odd hydrogen- and nitrogen-oxides. Production of  $\text{HO}_x$  (e.g.,  $\text{H}$ ,  $\text{OH}$ ,  $\text{HO}_2$ ) and  $\text{NO}_y$  (e.g.,  $\text{N}$ ,  $\text{NO}$ ,  $\text{NO}_2$ ,  $\text{NO}_3$ ) and depletion of  $\text{O}_3$  by solar proton events has been studied through both satellite observations and computational modeling (e.g., Cnutzen [1975]; Heath et al. [1977]; Reagan et al. [1981]; Jackman & McPeters [1985]; Jackman et al. [2000, 2001]). Jackman & McPeters [2004] review much of the work in this area.

The solar flare of 1 September 1859 was one of the most intense white-light flares ever observed [Tsunetani et al., 2003]. The flare itself was observed independently by Carrington [1860] and Hodgson [1860] and lasted approximately 5 minutes. The flare was followed about 17 hours later by a magnetic storm at the Earth which lasted about 2 hours [Carrington, 1860; Tsunetani et al., 2003]. The storm was of such intensity that in the United States and Europe res were started after arcing from induced currents in telegraph wires [loomis, 1861]. The storm was likely caused by energetic charged particles accelerated by one or several highly energetic coronal mass ejections (CME) from the Sun at the time of the flare. The geomagnetic activity associated with the accelerated particles lasted several days at least [Chapman & Bartels, 1940]. Studies of very energetic events associated with solar activity are important in understanding how such activity impacts various Earth-based systems. A n event as energetic as the 1859 one has not been modeled in this way before, and it may be that events of this magnitude and larger are not uncommon over the long term [Schaefer et al., 2000; Smith & Scob, 2007].

## 2. Methods

Our modeling was performed using the Goddard Space Flight Center two-dimensional atmospheric model that has

been used previously for modeling SPEs [Jackman et al., 1990, 2000, 2001, 2005a, b], as well as much higher energy events such as gamma-ray bursts [Thomas et al., 2005]. We briefly describe the model here. More detail on the version of the model used and its reliability for high fluence events is given by Thomas et al. [2005] and the appendix therein.

The model's two spatial dimensions are altitude and latitude. The latitude range is divided into 18 equal bands and extends from pole to pole. The altitude range includes 58 evenly spaced logarithmic pressure levels (approximately 2 km spacing) from the ground to approximately 116 km. The model computes 65 constituents with photochemical reactions, solar radiation variations, and transport (including winds and small scale mixing) as described by Thomas et al. [2005] and Fleming et al. [1999]. A photolytic source term is computed from a lookup table and used in calculations of photodissociation rates of atmospheric constituents by sunlight [Jackman et al., 1996].

We have employed two versions of the atmospheric model. One is intended for long term runs (many years) and includes all transport mechanisms (e.g., winds and diffusion); it has a time step of one day and computes daily averaged constituent values. The second is used for short term runs (a few days) and calculates constituent values throughout the day and night, but does not include full transport. This version has a time step of 225 seconds.

No direct measurements of the proton fluence are available from 1859, but an estimate of the fluence of this event based on measurements of nitrate enhancement in Greenland ice cores is given by McCracken et al. [2001a, b]. They use nitrate enhancements associated with events of known proton fluence (e.g. the 1972 and 1989 flares) to determine a scale factor between fluence and nitrate enhancement. This allows an estimate of fluence given a measured nitrate enhancement, with a range based on possible scale factor variation.

We assume a fluence of protons with energies greater than 30 MeV of  $27.4 \times 10^9 \text{ cm}^{-2}$  for the 1859 event, corresponding to the middle of the range of estimated values in McCracken et al. [2001a, b]. Given the known fluence of the October 1989 event ( $42 \times 10^9 \text{ cm}^{-2}$  [McCracken et al., 2001a]) the 1859 event was 6.5 times more energetic in protons. We use this value to scale up the computed atmospheric ionization profiles that were used by Jackman et al. [1995] to study effects of the October 1989 event for use in this study. This scaling is, of course, uncertain, since there is no way to know the specific proton spectrum for the 1859 event since this sort of data was not available before about 1955 [Svestka & Simon, 1975], but it is a "best guess" approach. A linear scaling seems appropriate, given that it has been shown for photon events of large fluence (which have similar atmospheric effects) that the production of nitrogen oxides ( $\text{NO}_y$ ) scales linearly with fluence, and the deposition of nitrate is directly dependent upon the  $\text{NO}_y$  production [Ejzak et al., 2007; Thomas et al., 2005]. While x-rays from the flare would be important in the upper atmosphere (above

about 70 km), they do not penetrate to the stratosphere and so have little or no impact on ozone [Barth et al., 1999; Hines et al., 1965]. We have therefore neglected any effects of x-rays.

The scaled-up ionization profiles are input to the short term version of the atmospheric model as a source of  $\text{NO}_y$  and  $\text{HO}_x$  which then go on to deplete ozone through catalytic cycles [Jackman & McPeters, 2004]. Several previous SPE studies have found that the proton flux is restricted to latitudes above about 60° [McPeters et al., 1981; Jackman et al., 2001, 2005b] by the Earth's magnetic field, the structure of which is modified by the SPE. We have no way of knowing the precise latitude restriction of the proton flux in the 1859 case, but we adopt the previous limit as likely.

We scale the whole range of ionization rates from the October 1989 event by a factor of 6.5, including ionizations that result from protons with energies between 1 and 30 MeV. The  $\text{HO}_x$  constituents, which are especially important above 50 km, are greatly impacted but have relatively short lifetimes and their effect is gone within several hours after the event is over.  $\text{NO}_y$  constituents above 50 km are increased by these lower energy protons and can be transported downwards to the upper stratosphere (below 50 km) during late fall and winter [Jackman et al., 2005b]. The largest stratospheric impact will be by those protons with energies greater than 30 MeV, because the  $\text{NO}_y$  produced by these high energy protons will be much deeper into the stratosphere where the lifetime of the  $\text{NO}_y$  family can be quite long (months in the middle stratosphere to years in the lower stratosphere).

While the main magnetic storm associated with the 1859 event was observed to last about 2 hours, the particle event likely occurred over several days, perhaps as many as 10 days. Most SPEs have durations of several days; the 1989 SPE from which we are extrapolating lasted 12 days. We have chosen to input ionization from the 1859 SPE over 2 days in our model. This duration may be shorter than the actual event, though we note that the magnetic storm had a short duration. This is a convenient duration for practical purposes with the model we used. It is known that long term atmospheric effects (e.g.: ozone depletion) from such ionization are much more strongly dependent on total fluence than on duration [Ejzak et al., 2007]. Therefore, we believe a difference in duration is not likely to yield significant changes to our conclusions. An expanded study could check this assertion in the context of proton events.

The total ionization is distributed over the 2 day duration uniformly (i.e.: as a step function) in the middle of a 7 day run of the short term model. Results of this run are then read in to the long term model which is run for several years to return the atmosphere to equilibrium, pre-event conditions.

### 3. Results

Our primary results are changes in  $\text{NO}_y$  and  $\text{O}_3$  in the stratosphere.  $\text{NO}_y$  is produced in the high latitude areas where the protons enter the atmosphere. Figure 1 shows the  $\text{NO}_y$  generated during and shortly after the event, as the percent difference in column  $\text{NO}_y$  between a run with the effect of the SPE included and one without. The maximum localized increase in column  $\text{NO}_y$  is about 240%.

Figures 2 and 3 show the percent difference in profile  $\text{NO}_y$  and  $\text{O}_3$ , respectively, between a run with the effect of the SPE included and one without, as a function of altitude and latitude, two months after the event. This is the point in time when the globally averaged ozone depletion is largest (see Figure 6). Note that the increased  $\text{NO}_y$  extends primarily upward in altitude from about 30 km and is most widespread in altitude at latitudes above about 30°. Also,

the  $\text{O}_3$  change is contained primarily within a band around 40 km altitude and restricted to latitudes above 30°.

Figure 4 shows the percent difference in column  $\text{NO}_y$  between a run with the effect of the SPE included and one without for four years after the event. As is apparent from this plot,  $\text{NO}_y$  is transported to some degree to mid and low latitudes, but remains primarily concentrated in the high latitude regions as the atmosphere recovers to its pre-event equilibrium.

Figure 5 shows percent difference in column  $\text{O}_3$  between a run with the effect of the SPE included and one without for four years after the event. The maximum localized decrease in  $\text{O}_3$  column density is about 14% and occurs in the high latitude areas where the  $\text{NO}_y$  increase is largest.

One may notice in Figures 1–5 that there is asymmetry between northern and southern hemisphere regions. This is because levels of  $\text{NO}_y$  and  $\text{O}_3$  vary seasonally, especially in the polar regions, due to variations in the presence and intensity of sunlight. Photolysis reactions play a critical role in the balance of constituents here and strongly affect the total values. A detailed discussion of these effects can be found in Thomas et al. [2005] for the case of a gamma-ray burst.

Figure 6 shows the globally averaged percent difference in ozone. The maximum decrease is about 5%, which occurs two months after the event. Maximum global ozone depletion is delayed as  $\text{NO}_y$  spreads and interacts with  $\text{O}_3$  over a larger area. This is quantitatively similar to the globally averaged anthropogenically-caused ozone depletion currently observed, which is predicted to diminish slowly over several decades [Möller, 2003]. By contrast, this naturally-caused ozone depletion from the 1859 solar flare is nearly gone in about four years.

Since we have estimated the intensity of the 1859 SPE using data from nitrate deposition in ice cores, a consistency check may be done by computing the nitrate rainout in the model. We have approached such a comparison in two ways.

First, the maximum localized enhancement over background in the model is about 14%, while the 1859 spike in Figure 1 of McCracken et al. [2001a] is about 200% over background. This is obviously a large disagreement. However, because nitrate deposition can be spotty and takes place over a period of months, we have also computed absolute deposition values. Adding up deposition in the model over three months following the flare, within the 10° latitude band centered at 75° North, yields a value of  $1360 \text{ ng cm}^{-2}$ . A similar computation following McCracken et al. [2001a, b], using the fluence value assumed above and a value of 30 for the conversion factor between fluence and nitrate deposition [McCracken et al., 2001a], gives  $822 \text{ ng cm}^{-2}$ , a factor of about 1.7 smaller than the model value.

We note that the difference between modeled and observed absolute deposition values is opposite that of the percent enhancement over background. That is, the percent enhancement in the model is smaller than that from the ice core data, while absolute values from the ice core data are smaller than in the model. Given the many sources of uncertainty the absolute comparison is at least reasonably close, being less than a factor of two different.

It is important to note that the percent enhancement comparison looks only at the height of the peak above background, while the absolute deposition value is effectively the area under that peak. A difference in how the nitrate is deposited over time could help explain this discrepancy. If in the actual event most of the nitrate was deposited in a relatively short amount of time compared to the model then the height of the peak would be greater, even if the area under that peak is less, as seen in our comparisons.

Similar comparisons have been done before with this model (Jackman et al., 1990; Thomas et al., 2005). Jackman et al. [1990] found that the model showed a smaller peak percentage enhancement of nitrates than did ice core results of Zeller et al. [1986] (around 10% from the model, compared to 400% from ice core). This discrepancy is of the same order as what we have found in this study and apparently indicates some scaling disagreement between the model computations and the observations.

#### 4. Conclusions

We find for the 1859 event an atmospheric impact appreciably larger than that of the most energetic are in the era of satellite monitoring, that of October 1989. Localized maximum column ozone depletion (see Figure 5) is approximately 3.5 times greater than that of the 1989 event (see Figure 3 of Jackman et al. [1995]). We note that this is a smaller factor than that relating the total energy of the two events (6.5). Ozone depletion has been seen in other contexts (e.g., gamma-ray burst impacts) to scale less than linearly with total energy (Thomas et al., 2005; Ejzak et al., 2007). Causes for this weaker dependence include: increased removal of important depletion species such as NO with increased levels of NO<sub>y</sub>; production of O<sub>3</sub> in isolated regions especially at lower altitudes which are normally shielded from solar UV which produces O<sub>3</sub>; and the "saturation" of depletion, where most of the O<sub>3</sub> in a given region is removed and so cannot be depleted any further.

Our nitrate deposition results do not show as dramatic an enhancement as the measurements by McCracken et al. [2001a]. This discrepancy does mirror a similar comparison between nitrate deposition as computed using this model and that measured in ice cores as described in Jackman et al. [1990]. This discrepancy may reflect differences in transport or deposition efficiency.

Finally, while the ozone depletion seen here is limited, even small increases in UVB can be detrimental to many life forms [Rousseaux et al., 1999; Cullen et al., 1992]. Flares of significantly larger energy have been observed on Sun-like stars [Schaefer et al., 2000], and may occur from time to time through the long history of life on Earth. (See Hallam & Wignall [2003] for an overview of terrestrial extinctions.) Such events would have more dramatic effects on the biosphere. Knowledge of the impacts of such flares is important in understanding the history of life here and possibly elsewhere, in particular on terrestrial planets around stars which are more active than the Sun.

Acknowledgments. This work was supported in part by the NASA Astrobiology: Exobiology and Evolutionary Biology Program under grant number NNG 04GM 14G at the University of Kansas.

#### References

- Barth, C. A., S. M. Bailey, & S. C. Solomon (1999), Solar-terrestrial coupling: Solar soft x-rays and thermospheric nitric oxide, *Geophys. Res. Lett.*, 26, 1251-1254.
- Carrington, R. C. (1860), Description of a singular appearance seen on the Sun on September 1, 1859, *Mon. Not. R. Astron. Soc.*, 20, 13-15.
- Chapman, S., & J. Bartels (1940), *Geomagnetism*, vol. I, pp. 328-337, Oxford Univ. Press, New York.
- Crutzen, P. J., et al. (1975), Solar proton events: Stratospheric sources of nitric oxide, *Science*, 189, 457-458.
- Cullen, J. J., P. J. Neale, & M. P. Lesser (1992), Biological Wighting Function for the Inhibition of Phytoplankton Photosynthesis by Ultraviolet Radiation, *Science*, 258, 646-649.
- Ejzak, L. M., A. L. M. Elliott, M. V. Medvedev, B. C. Thomas (2007), Terrestrial Consequences of Spectral and Temporal Variability in Ionizing Photon Events, *Astrophys. J.*, 654, 373.
- Fleming, E. L., C. H. Jackman, R. S. Stolarski, & D. B. Considine (1999), Simulation of stratospheric tracers using an improved empirically based two-dimensional model transport formulation, *J. Geophys. Res.*, 104, 23911-23934.
- Hallam, A., & P. Wignall (2003), *Mass Extinctions and their Aftermath*, Oxford Univ. Press, Oxford, UK.
- Hodgson, R. (1860), On a curious appearance seen in the Sun, *Mon. Not. R. Astron. Soc.*, 20, 15.
- Heath, D. F., et al. (1977), Solar proton event: influence on stratospheric ozone, *Science*, 197, 886-889.
- Hines, C. O., et al. (eds.) (1965), *Physics of the Earth's Upper Atmosphere*, 40 pp., Prentice-Hall, Englewood Cliffs, New Jersey.
- Jackman, C. H., & R. D. M. Peters (1985), The Response of Ozone to Solar Proton Events During Solar Cycle 21: A Theoretical Interpretation, *J. Geophys. Res.*, 90, 7955-7966.
- Jackman, C. H., A. R. Douglass, R. B. Rood, R. D. M. Peters, & P. E. Meade (1990), Effect of Solar Proton Events on the Middle Atmosphere During the Past Two Solar Cycles as Computed Using a Two-Dimensional Model, *J. Geophys. Res.*, 95, 7417-7428.
- Jackman, C. H., et al. (1995), Two-dimensional and three-dimensional model simulations, measurements, and interpretation of the influence of the October 1989 solar proton events on the middle atmosphere, *J. Geophys. Res.*, 100, 11641-11660.
- Jackman, C. H., E. L. Fleming, S. Chandra, D. B. Considine, & J. E. Rosenfeld (1996), Past, present, and future modeled ozone trends with comparisons to observed trends, *J. Geophys. Res.*, 101, 28753-28767.
- Jackman, C. H., E. L. Fleming, & F. M. Vitt (2000), Influence of extremely large solar proton events in a changing atmosphere, *J. Geophys. Res.*, 105, 11659-11670.
- Jackman, C. H., R. D. M. Peters, G. J. Labow, E. L. Fleming, C. J. Praderas, & J. M. Russell (2001), Northern Hemisphere atmospheric effects due to the July 2000 solar proton event, *Geophys. Res. Lett.*, 28, 2883-2886.
- Jackman, C. H., & R. D. M. Peters (2004), The effect of solar proton events on ozone and other constituents, *Geophysical Monograph*, 141, 305-319.
- Jackman, C. H., et al. (2005a), The Influence of the Several Very Large Solar Proton Events in Years 2000-2003 on the Neutral Middle Atmosphere, *Advances in Space Research*, 35, 445-450.
- Jackman, C. H., et al. (2005b), Neutral atmospheric influences of the solar proton events in October-November 2003, *J. Geophys. Res.*, 110, A09S27, doi:10.1029/2004JA.010888.
- Loomis, E. (1861), On the great auroral exhibition of Aug. 28th to Sept. 4, 1859, and on auroras generally, *Am. J. Sci.*, 82, 318.
- McCracken, K. G., G. A. M. Dreschhofer, E. J. Zeller, D. F. Smart, & M. A. Shea (2001a), Solar cosmic ray events for the period 1561-1994. 1. Identification in polar ice, 1561-1950, *J. Geophys. Res.*, 106, 21585-21598.
- McCracken, K. G., G. A. M. Dreschhofer, D. F. Smart, & M. A. Shea (2001b), Solar cosmic ray events for the period 1561-1994. 2. The Gleissberg periodicity, *J. Geophys. Res.*, 106, 21599-21609.
- M. Peters, R. D., C. H. Jackman, & E. G. Stassinopoulos (1981), Observations of ozone depletion associated with solar proton events, *J. Geophys. Res.*, 86, 12071-12081.
- Reagan, J. B., et al. (1981), Effects of the August 1972 solar particle events on stratospheric ozone, *J. Geophys. Res.*, 86, 1473-1494.
- Rousseaux, M. C., et al. (1999) Ozone depletion and UVB radiation: Impact on plant DNA damage in southern South America, *Proc. Nat. Acad. Sci. USA*, 96, 15310-15315.
- Schaefer, B. E., J. R. King, & C. P. Deliyannis (2000), Superflares on ordinary solar-type stars, *Astrophys. J.*, 529, 1026-1030.
- Smith, D. S., & J. Scalo (2007), Solar X-ray Flare Hazards on the Surface of Mars, *Planetary and Space Science*, in press.
- Svestka, Z., & P. Simon (1975) *Catalog of Solar Particle Events 1955-1969*, D. Reidel, Hingham, Mass.

Thomas, B., et al. (2005), Gamma-Ray Bursts and the Earth: Exploration of Atmospheric, Biological, Climatic and Biogeochemical Effects, *Astrophys. J.*, 634, 509-533.

Tsurutani, B.T., W.D. Gonzalez, G.S. Lakhina, & S. Alex (2003), The extreme magnetic storm of 1-2 September 1859, *J. Geophys. Res.*, 108 (A7), 1268, doi:10.1029/2002JA.009504.

Zeller, E.J., G.A.M. Dreschho, C.M. Laird (1986), Nitrate flux on the Ross Ice Shelf, Antarctica and its relation to solar cosmic rays, *Geophys. Res. Lett.*, 13, 1264-1267.

WMO (World Meteorological Organization) (2003), Scientific Assessment of Ozone Depletion: 2002, Global Ozone Research and Monitoring Project - Report No. 47, Geneva.

B.C. Thomas, Department of Physics and Astronomy, Washburn University, 1700 SW College Ave., Topeka, KS 66621, USA. (brian.thomas@washburn.edu)

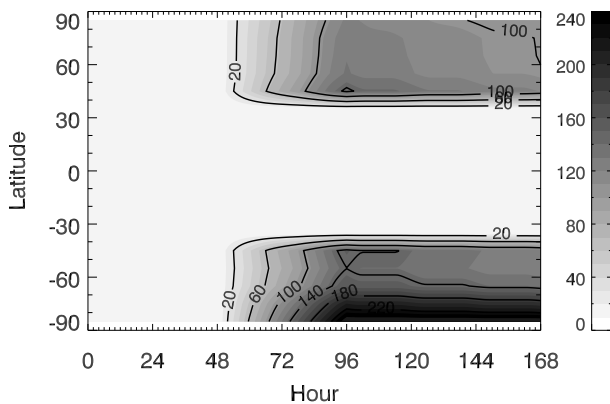


Figure 1. Percent difference in column  $\text{NO}_y$  between perturbed and unperturbed runs during the week in which the SPE occurs.

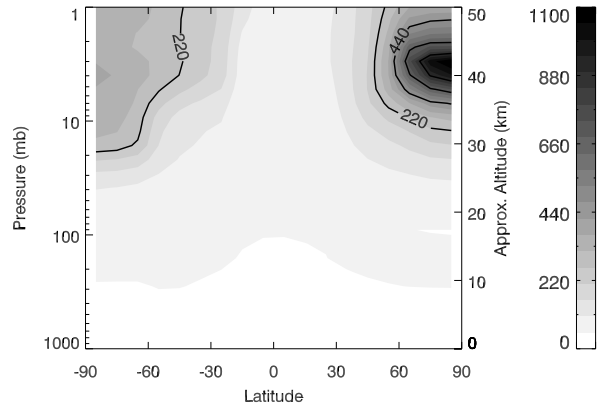


Figure 2. Percent difference in profile  $\text{NQ}$  between perturbed and unperturbed run, at two months after the event.

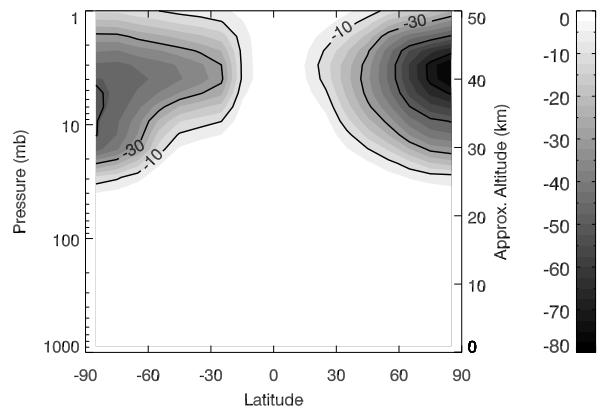


Figure 3. Percent difference in profile  $Q$  between perturbed and unperturbed run, at two months after the event.

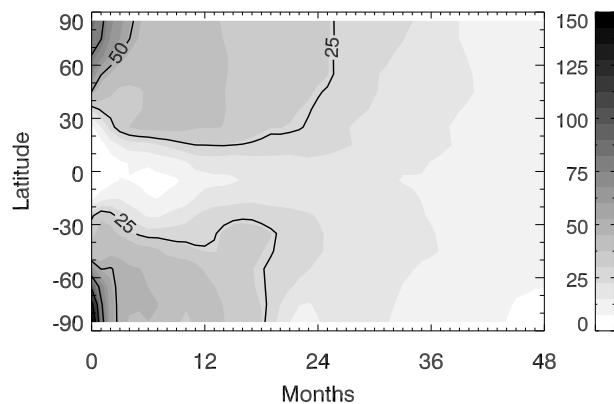


Figure 4. Percent difference in column  $\text{NO}_y$  between perturbed and unperturbed runs for the first four years after the SPE.

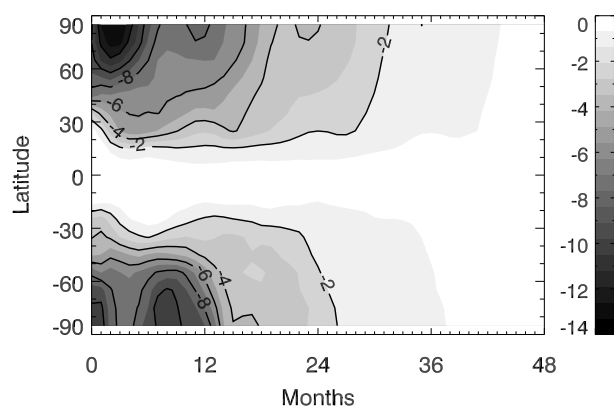


Figure 5. Percent difference in column  $\text{O}_3$  between perturbed and unperturbed runs for the first four years after the SPE.

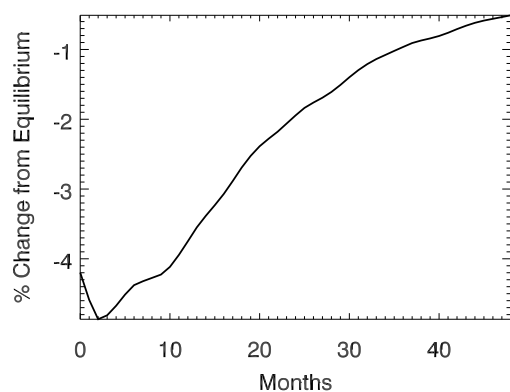


Figure 6. Globally averaged percent difference in column  $\text{O}_3$  between perturbed and unperturbed runs for the first four years after the SPE.